Canadian Conference - Pacific Conference on Earthquake Engineering 2023
Vancouver, British Columbia
June 25th – June 30th, 2023

Experimental Evaluation of Existing Exposed Column Base Plate Connections in Areas of Infrequent Seismic Activity in Eastern North America

Mohammad S. Akiel[1] and Colin A. Rogers[2*]

[1] PhD Candidate, Department of Civil Engineering, McGill University, Montréal, Canada
[2] Professor, Department of Civil Engineering, McGill University, Montréal, Canada
[*]colin.rogers@mcgill.ca (Corresponding Author)

ABSTRACT

An experimental program was conducted to assess the cyclic performance of existing column base plate connections in steel partial moment-resisting frames in areas with infrequent earthquakes in Eastern North America. The program comprised two 2-anchor and two 4-anchor rod connections, one of which considered steel corrosion. The connections were subjected to a symmetric cyclic lateral loading and a constant axial load.

The connections showed plastic deformation in the anchor rods and base plates. The plastic deformations were more evident in connections comprising four anchor rods. The direction of initial loading impacted the shape of the hysteresis in the moment-rotation relation curves for connections with two anchor rods. Specimens comprising four anchor rods showed approximately 58% and 56% larger ultimate and yielding moments, respectively. Energy dissipation was not affected by the number of anchor rods in the elastic loading stage. The 4-anchor rods connections, however, exhibited much higher cumulative energy dissipation capacities at the end of the testing.

Specimens that incorporated a reduction in the diameter of the anchor rods, due to anticipated corrosion, experienced slightly earlier yielding moments compared to their counterpart specimens. The effect of a reduced cross-section of the anchor rods on the energy dissipation capacity was more pronounced in the 2-anchor rod specimens. This could be ascribed by the fact that the anchor rods were the main contributor to the plastic deformations in the 2-anchor rod specimens.

Keywords: Existing steel structures, exposed base plate, cyclic loading, anchor rods, moment-rotation.

INTRODUCTION AND BACKGROUND

Column base plate connections are a critical component of steel structures, providing a means to transfer forces from the structure to the underlying foundations. There are three types of column base plate connections: exposed, shallow embedded, and deep embedded. Exposed column base plate connections showed popularity in low- to mid-rise steel structures due to their cost-effectiveness and ease of construction. However, the behaviour of these connections under axial and flexural loadings has been a topic of ongoing research. Grauvilardell et al. [1] conducted a comprehensive review on the work done on column base connections in the late century. They highlighted the importance of this topic and the need for further studies to improve the understanding of these structural elements and their response to seismic events. A study by Gomez [2] focused on characterizing the behaviour of exposed column base plate connections that are part of the current design practice in the United States. The shear transfer mechanisms and performance of seven connections under axial and flexural loadings were investigated. Kanvinde et al. [3] developed an analytical approach to evaluate the rotational stiffness of exposed column base connections when subjected to large moment-to-axial load ratios. Rodas et al. [4] developed a hysteretic model that can be implemented in numerical simulations of exposed column base connections. The model requires 16 parameters to be defined, four of which characterize the strength and stiffness of the connection, and the other 12 parameters, which must be calibrated by experiments, define the additional hysteretic rules such as the pinching, recentering of the column, and strength and/or stiffness deterioration. More recently, researchers have investigated the behaviour of column base connections in the weak direction [5-6]. Kabir [7] developed an approach, using machine learning, to identify the failure mode of exposed column base connections under combined axial and biaxial bending. On other hand, researchers have proposed the use of new techniques and materials to enhance the response of the newly constructed connections. Hassan et al. [8], for instance, tested four full-scale exposed column base connections comprising anchor rods (ARs) that incorporated a smooth shank with a reduced diameter covered with polyethylene. They claimed that their approach allowed for the strains to be distributed along the isolated shanks, hence preventing the failure in the connection, while preserving a desired ductile performance in the column base connections. It should be noted that, most of aforementioned studies have focused on newly constructed column base plate connections. Comparatively little attention has been given to the evaluation of the column base plate connections in existing steel structures, particularly in areas with infrequent seismic events. It is important to investigate the performance of these connections under a range of conditions to ensure that they can withstand seismic loading. Picard and Beaulieu [9], for example, conducted a series of tests on standard exposed column base plate connections, and they found that the connections developed considerable base fixity, which was contrary to the design assumption of zero "pinned" fixity that was common at the time. Seismic events, such as the Northridge and Kobe earthquakes, have highlighted the vulnerability of existing exposed column base plate connections to damage. Tremblay et al. [10] reported severe damage to these connections in the aftermath of these earthquakes, despite their assumed ability to withstand seismic loading. The development of seismic design provisions and standards, such as the National Building Code of Canada (NBCC) [11] and the Canadian Standards Association (CSA) Design of Steel Structures S16-19 [12] standard, has increased the uncertainty as how the past common practices and design philosophies will stand in an earthquake. Moreover, engineers involved in the assessment and retrofitting of existing steel structures are required to perform nonlinear response history analysis. Experimental data on column base plate connections are crucial for this purpose, and will be used to calibrate numerical models used in the evaluation. To this end, four column base connections with two or four anchor rods were tested to characterize their cyclic performance. These connections were popular in existing steel structures in Eastern North America before the 1990s. The test results should close some gaps in the literature, improve our understanding on the exposed column base plate connections, and assist in calibrating numerical models used in the evaluation of existing steel structures.

LABORATORY TEST PROGRAM

The laboratory program involved conducting tests on four steel column base plate connections, specifically W310 × 79 ASTM A572 GR 50 columns welded to CSA G40.21 300W base plates. The isometric view of a 2-anchor rod specimen can be seen in Figure 2. The test setup, which comprised vertical and horizontal actuators, is illustrated in Figure 1. The vertical actuator had an 11.4 MN compressive load capacity and an 8 MN tensile capacity with a displacement range of ±150 mm. Whereas the horizontal actuator had a ±1 MN and ±250 mm load and displacement capacities, respectively. Various sources were investigated to detail the specimens and to define their properties, including the length and shape of the anchor rods, the spacing between the anchor rods and the base plate edges, and the thickness of the base plate and grout layer. These sources included a literature review, a design standard from Dominion Bridge, a prominent engineering firm from before the 1990s, and plans of existing steel structures collected from several consulting firms in Montreal. The specimens were divided into two groups, 2-anchor rod and 4-anchor rod, based on the number of anchor rods, as listed in Table 1. The connections were subjected to a constant axial load equivalent to 20% P_y, where P_y is the cross-section yield force (i.e. $P_y = A_g F_y$), A_g is the cross-sectional area, and F_y is the nominal yield strength of the column. Furthermore, the specimens were subjected to varying lateral deformations based on the AISC 341 Standard [13] and Clark et al. [14] symmetric cyclic lateral loading protocol. The symmetric loading protocol was modified slightly by reducing the number of cycles to lessen the testing time, as shown in Figure 3. Each group comprised of two identical columns and base plates. Given that the test program aimed to target steel column base connections from the 1960s to 1990s, the expected corrosion of the anchor rods was considered in each group's connections, with one nominal and one corrosion-inclusive connection.

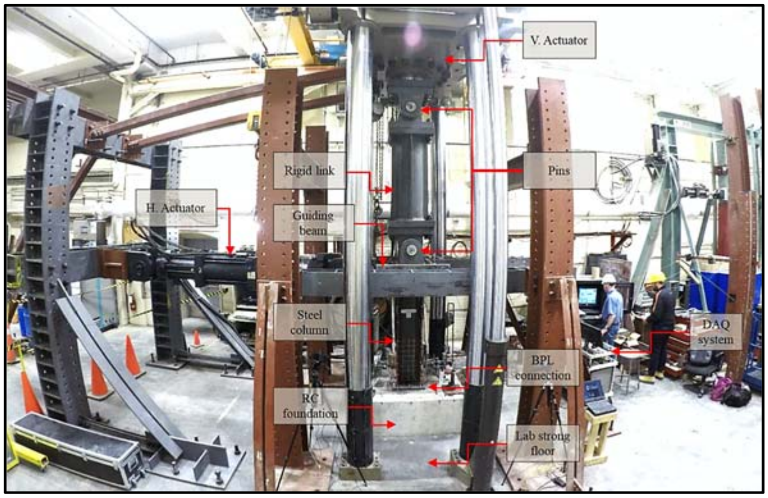

Figure 1: Testing setup

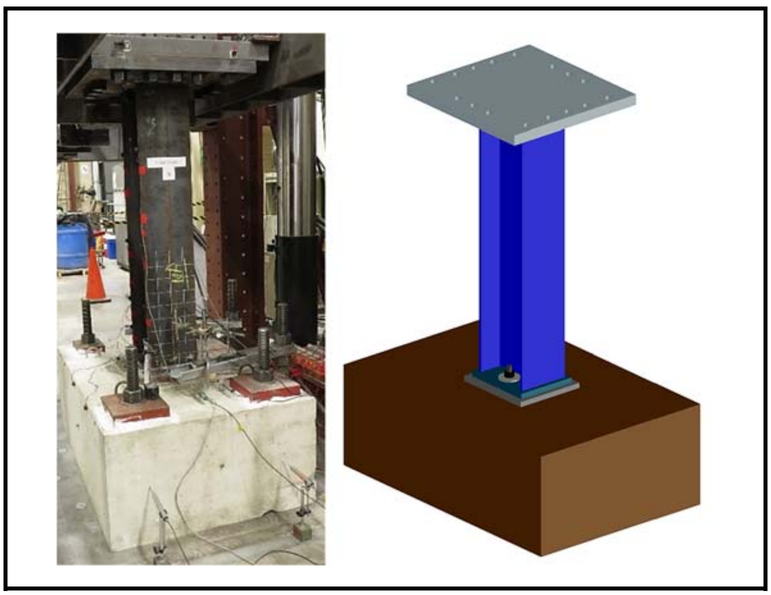

Figure 2: 3D view of a typical test specimen

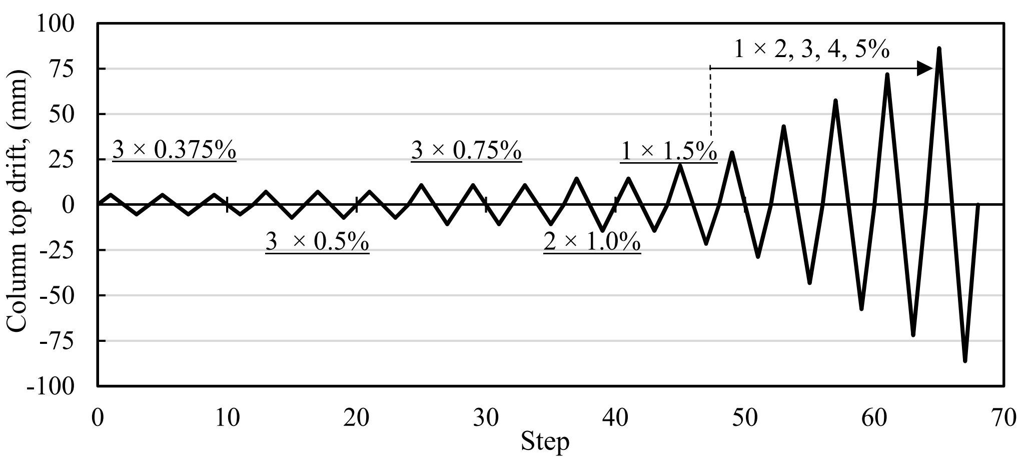

Figure 3: AISC symmetric cyclic lateral loading protocol, modified

Table 1: Test matrix

Group	Specimen	BPL dimension[a] (mm)	x-Spacing (mm)	y-Spacing (mm)
2-AR	2-AR-U[b]	300 × 350	-	150
	2-AR-C[c]	300 × 350	-	150
4-AR	4-AR-U	350 × 500	400	250
	4-AR-C	350 × 500	400	250

.[a] Dimension is given as width × length
.[b] Un-corroded anchor rods
.[c] Corroded anchor rods

The columns, with a clear length of 1360 mm, were connected to the 25.4 mm thick base plates using an all-around fillet weld of 8 mm thickness. It's worth noting that the all-around weld was not commonly used in the design of existing column base connections; however, the study of its influence on the connection was beyond the scope of the research. The top-end plates, 50.8 mm thick, were also welded to the columns and used to attach the specimens to the loading actuators. A 25.4mm non-shrink cementitious (SikaGrout® 212) grout layer [15] was poured between the column base plate and the underlying reinforced concrete (RC) foundation. L-shaped anchor rods were utilized in the testing program, as they were not commonly cited in the literature, but were prevalent in the reviewed old structural plans. There were no leveling nuts under the base plate, and instead, the vertical and horizontal actuators were utilized to establish the column leveling. The column bases were supported by RC foundations, and these foundation blocks were connected to the strong floor of the structures lab using 50.8mm high-strength steel threaded rods and plates. The nuts of the high-strength threaded rods were tightened using a hydraulic wrench, generating a total of 1000 kN vertical force on the RC foundations to prevent any movement during testing.

The method used to consider the material loss caused by corrosion was based on the approach presented by Andrade et al. [16]. They established an empirical correlation between the current density i_{corr}, which is defined as the average annual corrosion current per unit anodic surface area of steel in μA/cm^2, and the volume of steel consumed at the anode to determine the volume of rust produced at the anode. Specifically, the reduced diameter $D_{rb}(t)$ of a steel bar with an initial diameter of D_b (mm) that undergoes corrosion for a duration of Δ_t (in years) is given by

$$D_{rb} = D_b - 0.023\, i_{corr}\, \Delta_t \tag{1}$$

A time period of Δ_t = 43 years was assumed, corresponding to the time span from 1975 (the average between 1960 and 1990) to 2018 (the year of testing). The initial diameter D_b was 25.4 mm, and an i_{corr} value of 1.2, recommended by Celarec et al. [17] was used. Figure 4 shows the detailing of the reduced section of the anchor rod to account for the corrosion.

The steel columns arrived pre-welded to the end-plates from the supplier and were equipped with instrumentation before being connected to the RC foundation through the anchor rods. A ready-mix concrete was used to construct the RC foundation blocks. Figure 5.a and Figure 5.b show the formworks and steel cages before concrete casting for the 2-anchor rod and 4-anchor rod specimens, respectively. Figure 6 shows the RC blocks after concrete casting.

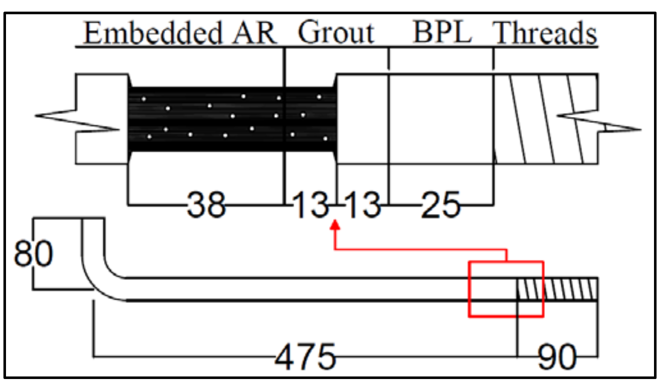

Figure 4: L-Shaped anchor rod detailing, dimensions in mm

(a) (b)

Figure 5: Formwork and steel cages prior to casting: (a) 2-anchor rod and (b) 4-anchor rod

Figure 6: RC Foundation blocks post concrete casting

MATERIAL

The mechanical properties of the materials used in the test were assessed. The base plate, anchor rods, and the column's web and flange coupons were tested before conducting the primary test on the column base connections. During the main testing, the concrete cylinders and beams that were cast with the RC foundation blocks were also tested. The average of the column's depth, *d*, was found to be 305.5 mm. The average thicknesses of the column's webs, t_w, and the flanges, t_f, were found to be 8.9 mm and 14.2 mm, respectively, whereas the flange width, b_f, was 252.2 mm. The average of the thickness of the base plates was 25.4 mm. The average value of the diameter for the anchor rods was 25.4 mm. Table 2 summarizes the deduced mechanical properties from the uniaxial tensile testing. The mechanical properties of the concrete material were evaluated in accordance with the concrete design standard CSA A23-14 [18]. Cylinders measuring 100 mm in diameter and 200 mm in length were used to evaluate the compression and split-tensile strengths of the concrete as specified in CSA A23.3-9C [19] and CSA A23.3-13C [20], respectively. The modulus of fracture of the concrete was determined using four-point bending tests, which were carried out with rectangular beams measuring 100 mm in depth, 100 mm in width, and 300 mm in length in accordance with A23.3-8C [21]. The mechanical properties of the concrete, including the compression strength, split-tensile strength, and modulus of fracture, were found to be 36.7 MPa, 4.04 MPa, and 3.15 MPa, respectively. The non-shrink cementitious grout (SikaGrout® 212) layer used between the base plate and the RC foundation had an average compressive strength of 56.9 MPa, which was evaluated using 50 × 50 × 50 mm cubes.

Table 2: Measured material properties

Material	***D-t*** (mm)	***E*** (GPa)	F_y (MPa)	ε_y %	F_u (MPa)	ε_u %	ΔL %
Anchor rod	25.4	209	321	0.15	485	19.13	26.8
Column web	8.9	207	385	0.18	474	17.30	25.1
Column flange	14.2	191	360	0.18	467	18.05	27.2
Base plate	25.4	203	444	0.22	531	12.93	22.9

MODE OF FAILURE

The 4-anchor rod specimens experienced a similar type of failure during testing. The failure began with the yielding of the anchor rods, followed by plastic deformations caused by the reversed cyclic demands. While the anchor rods did not completely fracture, their threads were damaged, as shown in Figure 7a, and the nuts slipped, leading to a sudden loss of load carrying capacity. The base plate also underwent permanent deformation due to flexural demands (Figure 7b), and cracks developed in the grout and concrete footing, but there was no concrete crushing. Yielding was observed at the bottom of the columns (Figure 7c), but no plastic hinge formation occurred because of the rocking behaviour exhibited by this type of exposed column base connection. The 2-anchor rod specimens exhibited a similar failure mode as the 4-anchor rod specimens, with plastic deformations in the anchor rods, but less pronounced elongation due to smaller tensile demands. The base plates of the 2-anchor rod specimens did not show noticeable plastic deformations, possibly due to the shorter overhang length. The columns' web did not exhibit yielding waves, and the anchor rods' threads did not show the damage observed in the 4-anchor rod specimens.

MOMENT-ROTATION RELATIONSHIP

The moment-rotation curves demonstrate the flag-shaped hysteresis resulting from the plastic deformation in the anchor rods and the gap formation between the base plate and the grout layer. Figure 8 and Figure 9 illustrate the moment-rotation curves of 4-AR-U and 4-AR-C specimens, respectively. The hysteresis for the 4-anchor rod specimens appeared symmetric on both sides of loading. Figure 10 and Figure 11 depict the moment-rotation relation of specimens 2-AR-U and 2-AR-C, respectively. Conversely, the loading history affected the hysteresis for the 2-anchor rod specimens. For example, the 2-AR-U specimen had loading starting in the positive direction, resulting in a moment value of 148 kN.m at +0.02 rad rotation. In contrast, the moment value was 138 kN.m at -0.02 rad. The 2-AR-C specimen was loaded in the negative direction and then the positive direction, leading to a smaller area in the flag-shape hysteresis for the positive direction in comparison to the negative direction. It is worth noting that the 2-AR-U specimen was tested twice at 30% and 20% of P_y, and the results presented here are from the second test, which was at 20% P_y, explaining the symmetry of the positive and negative hysteresis. The 4-AR specimens showed approximately 58% and 56% increase in the ultimate, M_m, and the yielding, M_y, moment values, respectively, compared to the 2-anchor rod specimens. This increase is justified by the location of the anchor rods and their distance from the neutral axis, as well as the moment arm. The yielding moment is defined using the moment-rotation envelope; a line is drawn from the origin through a point corresponding to 75% of the peak moment on the moment-rotation envelope. A horizontal line is then drawn from the peak moment point, and a vertical line is drawn from the point where the initial and horizontal lines intersect to the moment-rotation envelope. The yielding point is the intersection of the vertical line and the moment-rotation envelope. Figure 12 illustrates this process, and Table 3 presents the key test results, including yielding moments and other data.

(a) (b) (c)

Figure 7: 4-anchor rod specimens' post-testing components

Table 3: Summary of test results

Specimen	Yielding						Peak			
	Positive (+)			Negative (−)			Positive (+)		Negative (−)	
	θ_y (%rad)	M_y (kN.m)	$k_y \times 10^3$ (kN.m/rad)	θ_y (%rad)	M_y (kN.m)	$k_y \times 10^3$ (kN.m/rad)	θ_m (%rad)	M_m (kN.m)	θ_m (%rad)	M_m (kN.m)
2-AR-U	0.54	119.4	22	0.62	123.2	20	2.48	151.7	1.84	150.2
2-AR-C	0.33	115.3	35	0.42	122.9	29	1.78	138.5	1.72	149.1
4-AR-U	0.63	187.7	30	0.91	192.6	21	2.82	233.4	3.30	241.5
4-AR-C	0.55	184.5	34	0.79	186.7	24	3.01	229.3	2.58	229.0

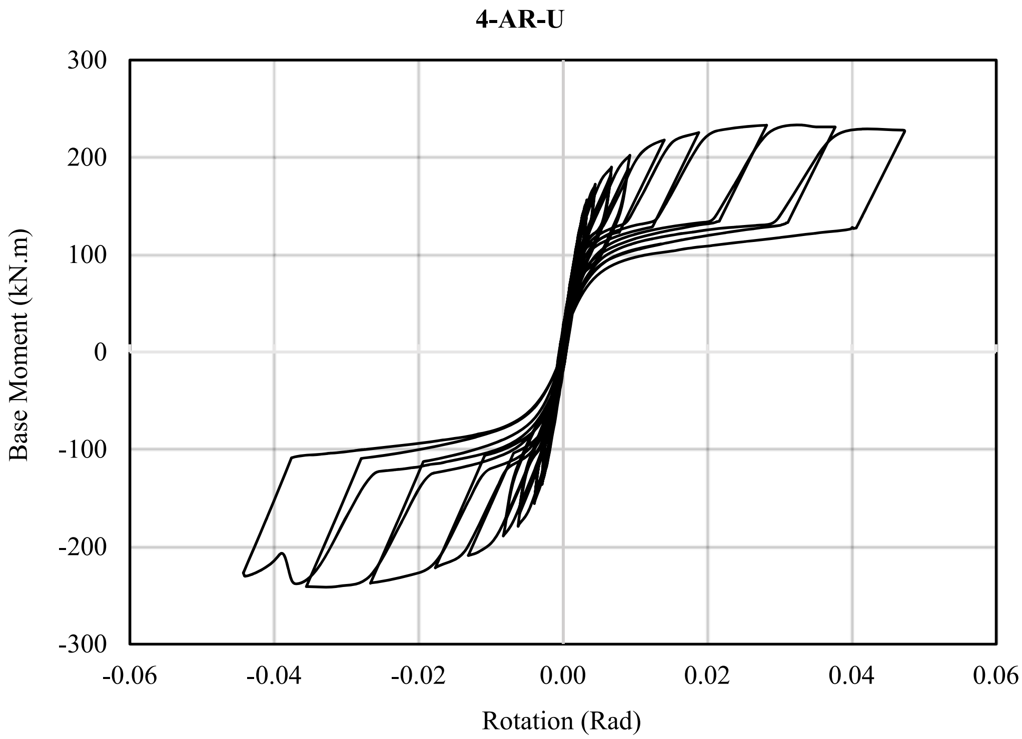

Figure 8: Moment-rotation relation for 4-AR-U specimen

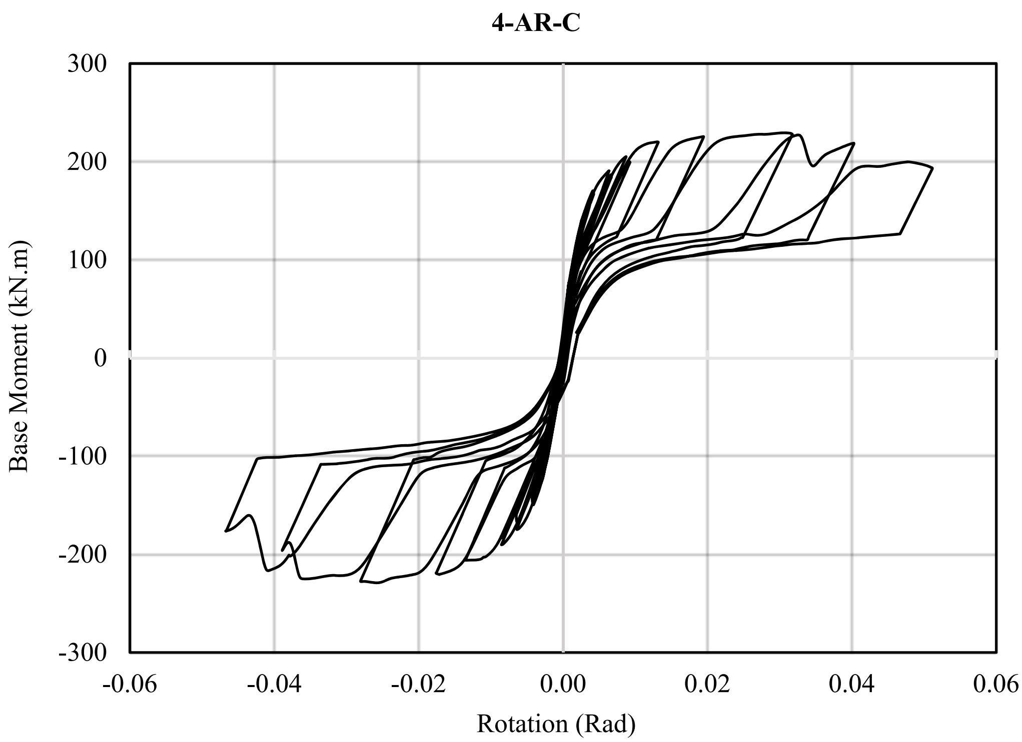

Figure 9: Moment-rotation relation for 4-AR-C specimen

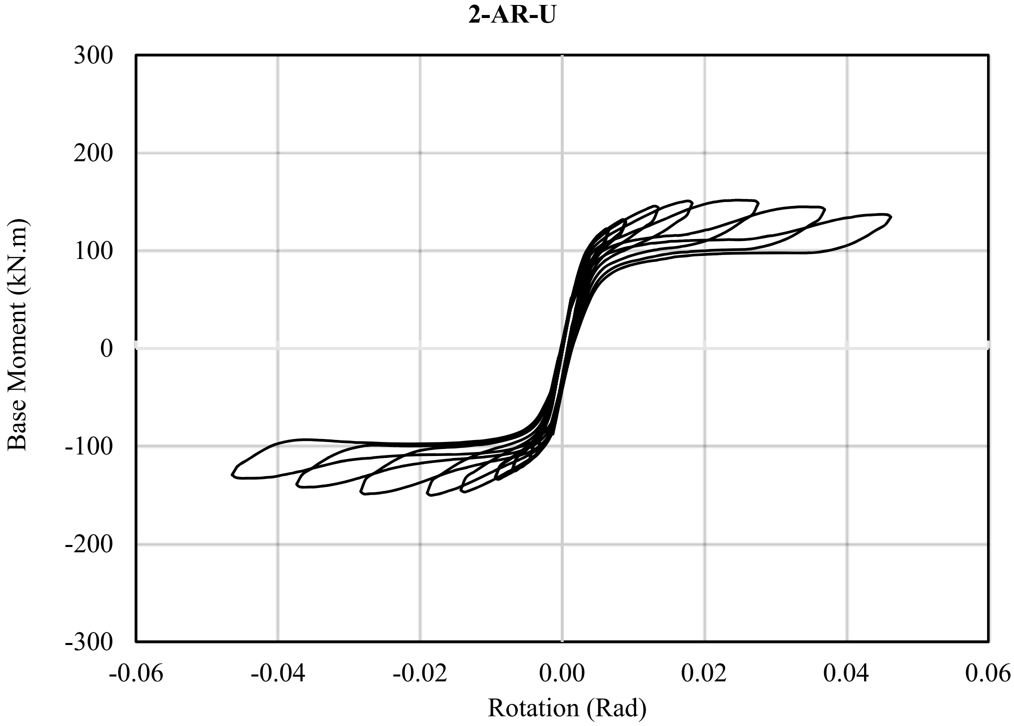

Figure 10: Moment-rotation relation for 2-AR-U specimen

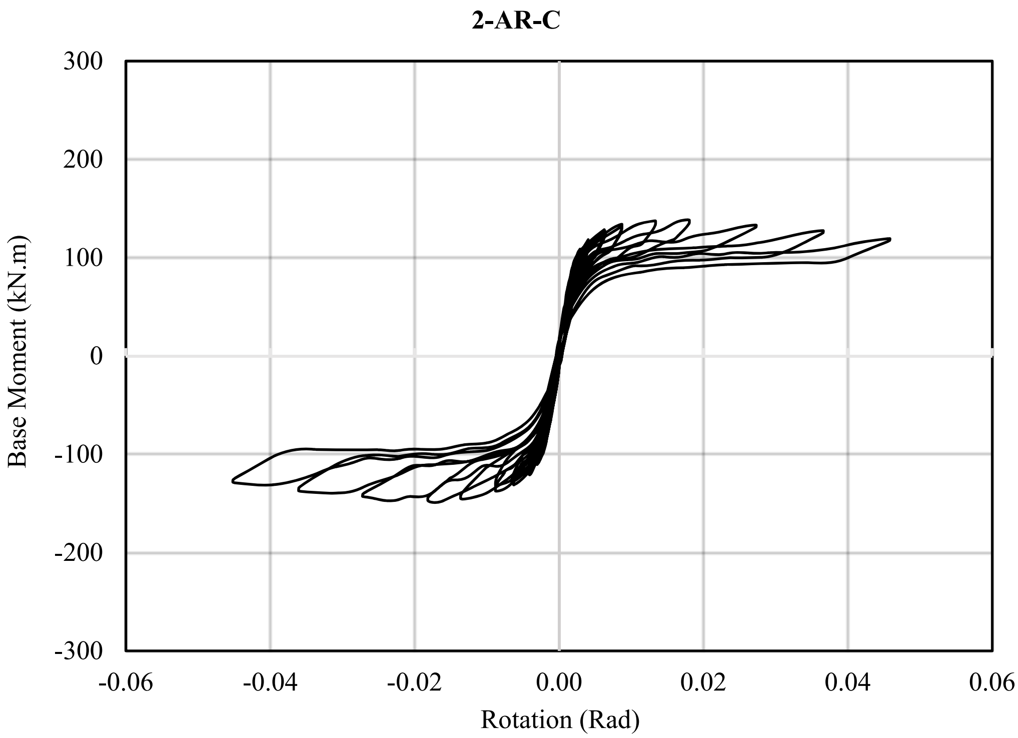

Figure 11: Moment-rotation relation for 2-AR-C specimen

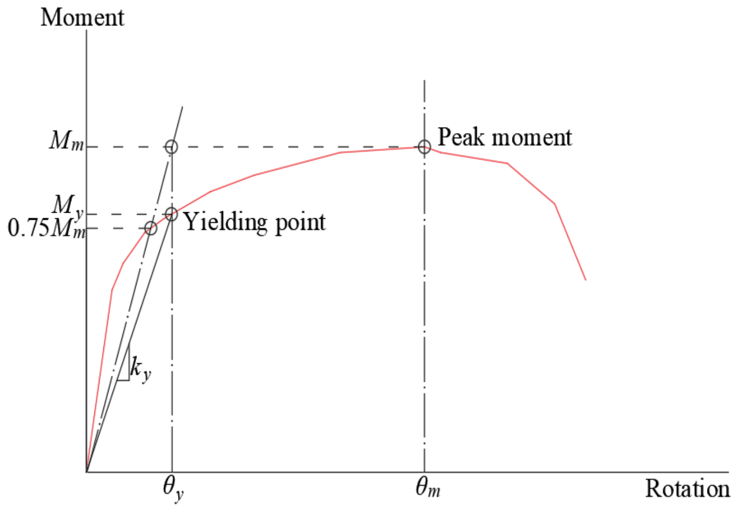

Figure 12: Definition of yielding point and initial stiffness, ky, on the M-θ envelop

DUCTILITY AND ENERGY DISSIPATION CAPACITY

Ductility is the ability of a structure to undergo inelastic deformations. To determine the ductility, one can calculate the ratio of the deformation at failure to the deformation at the onset of yielding. The ductility factors of the tested specimens are shown in Figure 13, where the factor is the ratio of the base rotation at peak moment to the rotation at yielding. All specimens exhibited a minimum ductility factor of 3 and 4 for negative and positive loading directions, respectively. Anchor rods in specimens that accounted for corrosion showed higher ductility factors compared to those without corrosion, possibly due to the reduced section and earlier yielding in those specimens. To determine the energy dissipation capacity, the enclosed area of the first cycle per aimed rotation angle was calculated from the moment-rotation curve. Figure 14 illustrates the cumulative energy dissipation capacity, which was computed by adding the energy dissipation capacity from zero to the aimed rotation angle. The dissipated energy per cycle is depicted in Figure 15. All specimens displayed a comparable energy dissipation capacity prior to the onset of yielding. However, the effect of corrosion became more evident in the 2-anchor rod specimens when yielding occurred. This could be attributed to the fact that the anchor rods were the primary contributor to the plastic deformations in the 2-anchor rod specimens, resulting in greater energy dissipation in the 2-AR-U specimen compared to the 2-AR-C specimen. For example, at a 5% rotation angle, the difference between the cumulative dissipated energy of the 2-AR-U and 2-AR-C specimens was 47%. In contrast, other components of the connections were involved in the plastic deformation of the 4-anchor rod specimens, as explained in the mode of failure section. Therefore, the 4-AR-U and 4-AR-C specimens had almost the same energy dissipation capacity at the end of the test.

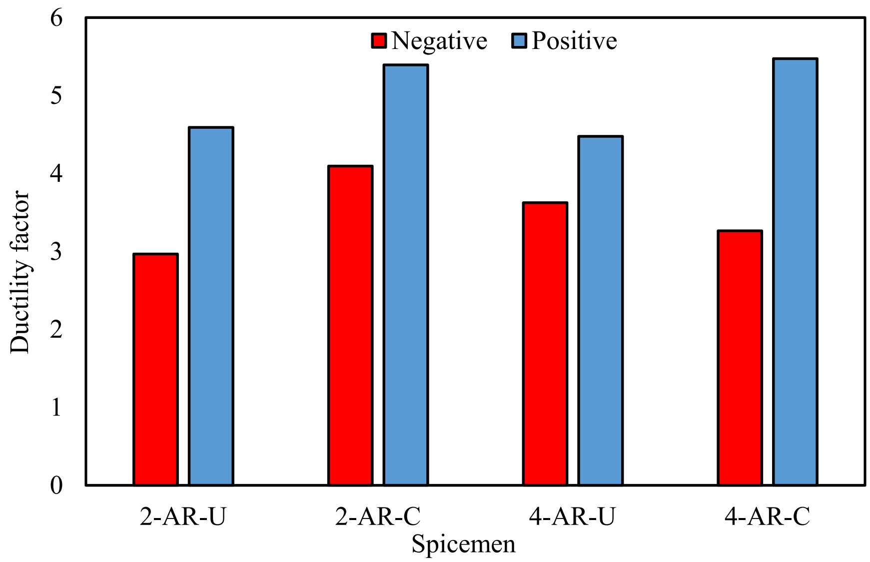

Figure 13: Ductility factors of the tested specimens

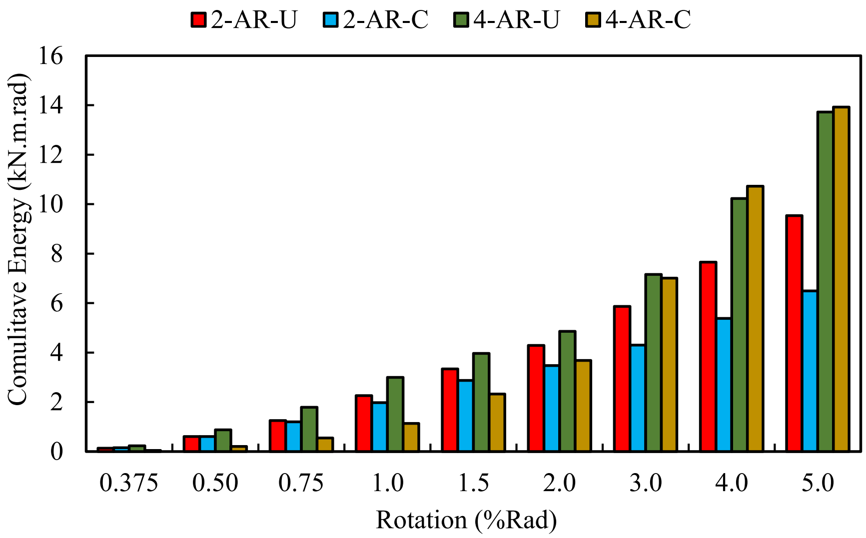

Figure 14: Cumulative energy dissipation capacity of the tested specimens

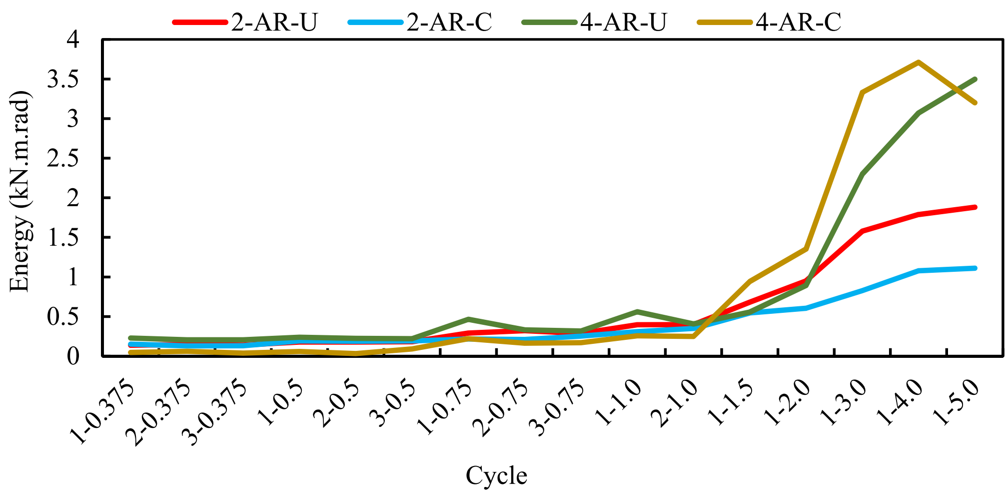

Figure 15: Dissipated energy per cycle

SUMMARY AND CONCLUSIONS

The behaviour of standard column base plate connections used in low- to mid-rise steel structures in zones that experience infrequent seismic activities in Eastern North America was studied. Reversed cyclic tests on four exposed column base plate connections were conducted, each comprising two or four L-shape anchor rods. The influence of anchor rod corrosion on the cyclic performance of the connections was investigated. The study analyzed various aspects of the connections, such as their mode of failure, moment-rotation relationship, ductility, and energy dissipation capacity, leading to the following conclusions:

1. All specimens experienced plastic deformations in the anchor rods and pinch and slip hysteresis. The 4-anchor rod specimens experienced plastic deformations in their base plate and damage in the anchor rods' threads, which resulted in sudden drops of the load carrying capacity.
2. The 4-anchor rod specimens developed a symmetric hysteresis; nonetheless, the hysteresis of the 2-anchor rod specimens was asymmetric and was affected by the initial direction of loading.
3. Specimens comprising anchor rods that accounted for the corrosion effects (i.e., 2-AR-C and 4-AR-C) demonstrated smaller base rotation angles at yielding compared to their counterpart specimens; consequently, they showed higher ductility factors.
4. All specimens were able to dissipate energy through inelastic deformations. The anchor rods' corrosion effect on the energy dissipation capacity was more pronounced in the 2-anchor rod specimens. Whereas the 4-anchor rod specimens exhibited almost the same cumulative energy dissipation capacity at the end of the testing.

ACKNOWLEDGMENTS

The authors would like to acknowledge the financial support provided by the Natural Sciences and Engineering Research Council of Canada (NSERC), the Fonds de recherche du Québec – Nature et technologies (FRQ-NT), and the Centre d'études interuniversitaire des structures sous charges extrêmes (CEISCE). The Faculty of Engineering at McGill University provided the first author with a McGill Engineering Doctoral Award. Fabrication and supply of the steel components and anchor rods was carried out by Groupe Acier CAMNOR.

REFERENCES

[1] Grauvilardell, Jorge E, Daeyong Lee, Jerome F Hajjar, and Robert J Dexter. (2005). *Synthesis of design, testing and analysis research on steel column base plate connections in high-seismic zones*, Structural engineering report no. ST-04-02. Minneapolis (MN): Department of Civil Engineering, University of Minnesota.

[2] Gomez, Ivan Ricardo. (2010). "Behavior and design of column base connections", University of California, Davis.

[3] Kanvinde, AM, DA Grilli, and F Zareian. (2012). "Rotational stiffness of exposed column base connections: Experiments and analytical models", *Journal of Structural Engineering*, 138: 549-60.

[4] Rodas, Pablo Torres, Farzin Zareian, and Amit Kanvinde. (2016). Hysteretic model for exposed column–base connections, *Journal of Structural Engineering*, 142: 04016137.

[5] Lim, Woo-Young, Dongkeun Lee, and Young-Chan You. (2017). "Cyclic loading tests on exposed column-base plate weak-axis connections of small-size steel structures", *Engineering Structures*, 153: 653-64.

[6] Hassan, Ahmad S, Pablo Torres-Rodas, Laura Giulietti, and Amit Kanvinde. (2021). "Strength characterization of exposed column base plates subjected to axial force and biaxial bending", *Engineering Structures*, 237: 112165.

[7] Kabir, Md Asif Bin. (2021). "Behavior of exposed column base plate connection subjected to combined axial load and biaxial bending".

[8] Hassan, Ahmad S, Biao Song, Carmine Galasso, and Amit Kanvinde. (2022). "Seismic Performance of Exposed Column–Base Plate Connections with Ductile Anchor Rods", *Journal of Structural Engineering*, 148: 04022028.

[9] Picard, A, and D Beaulieu. (1985). "Behaviour of a simple column base connection", *Canadian Journal of Civil Engineering*, 12: 126-36.

[10] Tremblay, Robert, André Filiatrault, Peter Timler, and Michel Bruneau. (1995). "Performance of steel structures during the 1994 Northridge earthquake", *Canadian Journal of Civil Engineering*, 22: 338-60.

[11] National Building Code of Canada - NBCC. (2020). National Research Council of Canada: Ottawa, ON.

[12] Canadian Standards Association - CSA (2019). *CSA S16-19: Design of Steel Structures*. Mississauga, ON, Canada.

[13] American Institute of Steel Construction - AISC (2016). *ANSI/AISC 341-16: Seismic Provisions for Structural Steel Building*, Chicago, IL, USA.

[14] Clark, P., Frank, K., Krawinkler, H. and Shaw, R. (1997). *Protocol for Fabrication, Inspection, Testing, and Documentation of Beam-Column Connection Tests and Other Experimental Specimens*, Report No. SAC/BD-97. SAC Joint Venture.

[15] SikaGrout® - 212. (2018). Sika Canada INC. Product Data Sheet: Pointe-Claire, QC

[16] Andrade, C, C Alonso, and FJ Molina. 1993. "Cover cracking as a function of bar corrosion: Part I-Experimental test", *Materials and structures*, 26: 453-64.

[17] Celarec, Daniel, Dimitrios Vamvatsikos, and Matjaž Dolšek. (2011). "Simplified estimation of seismic risk for reinforced concrete buildings with consideration of corrosion over time", *Bulletin of Earthquake Engineering*, 9: 1137-55.

[18] Canadian Standards Association - CSA (2014a). *CSA A23-14: Design of concrete structures.*, Rexdale, ON.

[19] Canadian Standards Association - CSA (2014b). *CSA A23.2-9C-14: Compressive Strength of Cylindrical Concrete Specimens,* Rexdale, ON.

[20] Canadian Standards Association - CSA (2014c). *CSA A23.2-13C-14: Splitting Tensile Strength of Cylindrical Concrete Specimens*, Rexdale, ON.

[21] Canadian Standards Association - CSA (2014d). *CSA A23.2-8C-14: Flexural Strength of Concrete (Using a Simple Beam with Third Point Loading)*, Rexdale, ON.